16. Katami M. Corneal transplantation-immunologically privileged status. *Eye.* 1991;5(5):528-548.
17. Dalton DK, Pitts-Meek S, Keshav S, Figari IS, Bradley A, Stewart TA. Multiple defects of immune cell function in mice with disrupted interferon-gamma genes. *Science.* 1993;259(5102):1739-1742.
18. Swihart K, Fruth U, Messmer N, et al. Mice from a genetically resistant background lacking the interferon gamma receptor are susceptible to infection with Leishmania major but mount a polarized T helper cell 1-type CD4+ T cell response. *J Exp Med.* 1995;181(3):961-971.
19. Nakae S, Komiyama Y, Nambu A, et al. Antigen-specific T cell sensitization is impaired in IL-17-deficient mice, causing suppression of allergic cellular and humoral responses. *Immunity.* 2002; 17(3):375-387.
20. Schwarzenberger P, La Russa V, Miller A, et al. IL-17 stimulates granulopoiesis in mice: use of an alternate, novel gene therapy-derived method for in vivo evaluation of cytokines. *J Immunol.* 1998;161(11):6383-6389.
21. Hori J, Joyce NC, Streilein JW. Immune privilege and immunogenicity reside among different layers of the mouse cornea. *Invest Ophthalmol Vis Sci.* 2000;41(10):3032-3042.
22. Klebe S, Coster DJ, Sykes PJ, et al. Prolongation of sheep corneal allograft survival by transfer of the gene encoding ovine IL-12-p40 but not IL-4 to donor corneal endothelium. *J Immunol.* 2005; 175(4):2219-2226.
23. Beauregard C, Stevens C, Mayhew E, Niederkorn JY. Cutting edge: atopy promotes Th2 responses to alloantigens and increases the incidence and tempo of corneal allograft rejection. *J Immunol.* 2005;174(11):6577-6581.
24. Hidalgo LG, Halloran PF. Role of IFN-gamma in allograft rejection. *Crit Rev Immunol.* 2002;22(4):317-349.
25. Halloran PF, Afrouzian M, Ramassar V, et al. Interferon-gamma acts directly on rejecting renal allografts to prevent graft necrosis. *Am J Pathol.* 2001;158(1):215-226.
26. Halloran PF, Miller LW, Urmson J, et al. IFN-gamma alters the pathology of graft rejection: protection from early necrosis. *J Immunol.* 2001;166(12):7072-7081.
27. Fallarino F, Grohmann U, Hwang KW, et al. Modulation of tryptophan catabolism by regulatory T cells. *Nat Immunol.* 2003;4(12): 1206-1212.
28. Zhang J. Yin and yang interplay of IFN-gamma in inflammation and autoimmune disease. *J Clin Invest.* 2007;117(4):871-873.
29. Wang Z, Hong J, Sun W, et al. Role of IFN-gamma in induction of Foxp3 and conversion of CD4+ CD25- T cells to CD4+ Tregs. *J Clin Invest.* 2006;116(9):2434-2441.
30. Sawitzki B, Kingsley CI, Oliveira V, Karim M, Herber M, Wood KJ. IFN-gamma production by alloantigen-reactive regulatory T cells is important for their regulatory function in vivo. *J Exp Med.* 2005; 201(12):1925-1935.
31. Guillonneau C, Hill M, Hubert FX, et al. CD40Ig treatment results in allograft acceptance mediated by CD8CD45RC T cells, IFN-gamma, and indoleamine 2,3-dioxygenase. *J Clin Invest.* 2007; 117(4):1096-1106.
32. Steinman L. A brief history of T(H)17, the first major revision in the T(H)1/T(H)2 hypothesis of T cell-mediated tissue damage. *Nat Med.* 2007;13(2):139-145.
33. Nakae S, Suto H, Berry GJ, Galli SJ. Mast cell-derived TNF can promote Th17 cell-dependent neutrophil recruitment in ovalbumin-challenged OTII mice. *Blood.* 2007;109(9):3640-3648.
34. Nakae S, Iwakura Y, Suto H, Galli SJ. Phenotypic differences between Th1 and Th17 cells and negative regulation of Th1 cell differentiation by IL-17. *J Leukocyte Biol.* 2007;81(5):1258-1268.
35. Lubberts E. IL-17/Th17 targeting: on the road to prevent chronic destructive arthritis?. *Cytokine.* 2008;41(2):84-91.
36. Lim HW, Lee J, Hillsamer P, Kim CH. Human Th17 cells share major trafficking receptors with both polarized effector T cells and FOXP3+ regulatory T cells. *J Immunol.* 2008;180(1):122-129.
37. Su SB, Grajewski RS, Luger D, et al. Altered chemokine profile associated with exacerbated autoimmune pathology under conditions of genetic interferon-gamma deficiency. *Invest Ophthalmol Vis Sci.* 2007;48(10):4616-4625.
38. Cox CA, Shi G, Yin H, et al. Both Th1 and Th17 are immunopathogenic but differ in other key biological activities. *J Immunol.* 2008;180(11):7414-7422.
39. Luger D, Silver PB, Tang J, et al. Either a Th17 or a Th1 effector response can drive autoimmunity: conditions of disease induction affect dominant effector category. *J Exp Med.* 2008;205(4):799-810.
40. Kobayashi T, Okamoto S, Hisamatsu T, et al. IL-23 differentially regulates the Th1/Th17 balance in ulcerative colitis and Crohn's disease. *Gut.* 2008;57(12):1682-1689.
41. Afzali B, Lombardi G, Lechler RI, Lord GM. The role of T helper 17 (Th17) and regulatory T cells (Treg) in human organ transplantation and autoimmune disease. *Clin Exp Immunol.* 2007;148(1): 32-46.
42. Jones LS, Rizzo LV, Agarwal RK, et al. IFN-gamma-deficient mice develop experimental autoimmune uveitis in the context of a deviant effector response. *J Immunol.* 1997;158(12):5997-6005.
43. Flynn TH, Ohbayashi M, Ikeda Y, Ono SJ, Larkin DF. Effect of allergic conjunctival inflammation on the allogeneic response to donor cornea. *Invest Ophthalmol Vis Sci.* 2007;48(9):4044-4049.
44. Bishop DK, Chan Wood S, Eichwald EJ, Orosz CG. Immunobiology of allograft rejection in the absence of IFN-gamma: CD8+ effector cells develop independently of CD4+ cells and CD40-CD40 ligand interactions. *J Immunol.* 2001;166(5):3248-3255.
45. El-Sawy T, Miura M, Fairchild R. Early T cell response to allografts occurring prior to alloantigen priming up-regulates innate-mediated inflammation and graft necrosis. *Am J Pathol.* 2004;165(1): 147-157.
46. Miura M, El-Sawy T, Fairchild RL. Neutrophils mediate parenchymal tissue necrosis and accelerate the rejection of complete major histocompatibility complex-disparate cardiac allografts in the absence of interferon-gamma. *Am J Pathol.* 2003;162(2):509-519.
47. Surquin M, Le Moine A, Flamand V, et al. IL-4 deficiency prevents eosinophilic rejection and uncovers a role for neutrophils in the rejection of MHC class II disparate skin grafts. *Transplantation.* 2005;80(10):1485-1492.
48. Forlow SB, Schurr JR, Kolls JK, Bagby GJ, Schwarzenberger PO, Ley K. Increased granulopoiesis through interleukin-17 and granulocyte colony-stimulating factor in leukocyte adhesion molecule-deficient mice. *Blood.* 2001;98(12):3309-3314.
49. Miyamoto M, Prause O, Sjostrand M, Laan M, Lotvall J, Linden A. Endogenous IL-17 as a mediator of neutrophil recruitment caused by endotoxin exposure in mouse airways. *J Immunol.* 2003; 170(9):4665-4672.
50. George-Chandy A, Nordstrom I, Nygren E, et al. Th17 development and autoimmune arthritis in the absence of reactive oxygen species. *Eur J Immunol.* 2008;38(4):1118-1126.
51. Ohteki T, Fukao T, Suzue K, et al. Interleukin 12-dependent interferon gamma production by CD8alpha+ lymphoid dendritic cells. *J Exp Med.* 1999;189(12):1981-1986.
52. Yamada J, Maruyama K, Sano Y, Kinoshita S, Murata Y, Hamuro J. Promotion of corneal allograft survival by the induction of oxidative macrophages. *Invest Ophthalmol Vis Sci.* 2004;45(2):448-454.
53. Yamada J, Hamuro J, Terai K, Kinoshita S. Major histocompatibility complex semi-matching improves murine corneal allograft survival under oxidative macrophage dominancy. *Transplantation.* 2007; 84(7):899-907.

The Variation In Transparency Of Amniotic Membrane Used In Ocular Surface Regeneration

Che J Connon, James Doutch, Bo Chen, et al.

Br J Ophthalmol published online March 19, 2009
doi: 10.1136/bjo.2008.153064

BJO Online First, published on March 19, 2009 as 10.1136/bjo.2008.153064

The Variation In Transparency Of Amniotic Membrane Used In Ocular Surface Regeneration

C.J. Connon[1], J. Doutch[2], B. Chen[1], A. Hopkinson[3], J.S. Mehta[4], T. Nakamura[5], S. Kinoshita[5] and K.M. Meek[2].

[1] Dr Che John Connon (corresponding author)
School of Pharmacy, University of Reading, United Kingdom.
c.j.connon@reading.ac.uk
[2] School of Optometry & Vision Sciences, Cardiff University, UK
[3] Division of Ophthalmology & Visual Sciences, Queens Medical Centre, Nottingham, UK
[4] Singapore National Eye Centre, Singapore
[5] Department of Ophthalmology, Kyoto Prefectural University of Medicine, Japan

Keywords: amnion, transparency, collagen, refraction, cornea

Abstract

Background/aims: Scant consideration has been given to the variation in structure of human amniotic membrane (AM) at source or to the significance such differences might have on its clinical transparency. Therefore, we applied our experience of quantifying corneal transparency to AM.

Methods: Following elective caesarean, AM from areas of the fetal sac distal and proximal (i.e. adjacent) to the placenta was compared to freeze-dried AM. The transmission of light through the AM samples was quantified spectrophotometrically, also measured were tissue thickness by light microscopy and refractive index by refractometry.

Results: Freeze-dried and freeze-thawed AM samples distal and proximal to the placenta differed significantly in thickness, percent transmission of visible light and refractive index. The thinnest tissue (freeze-dried AM) had the highest transmission spectra. The thickest tissue (freeze-thawed AM proximal to the placenta) had the highest refractive index. Using the direct summation of fields method to predict transparency from an equivalent thickness of corneal tissue, AM was found to be up to 85% as transparent as human cornea.

Conclusion: When preparing AM for ocular surface reconstruction within the visual field, consideration should be given to its original location from within the fetal sac and its method of preservation, as either can influence corneal transparency.

Introduction

For several years *in vivo* and *in vitro*-based evidence has demonstrated the ability of amniotic membrane to provide a natural substrate upon which cells can grow[1-3]. Subsequently, human amniotic membrane (AM) is now firmly established as an important adjunct for ocular surface reconstruction across a broad spectrum of conditions[4] where it is often directly applied as a patch or a graft. For more serious conditions, such as limbal stem cell deficiency, AM taken from the fetal sac has also been employed as a substrate on to which donor corneal epithelial progenitor (limbal) cells are expanded, forming tissue engineered constructs suitable for surgical application[5]. However such therapeutic applications of AM often results in its post operative positioning within the visual field and sometimes, as in limbal stem cell transplantation, for prolonged or indefinite periods. In such cases the question of AM's transparency becomes crucial.

AM is the most structurally robust of the fetal membranes[6] consisting of a single layer of epithelial cells on a thick basement membrane which in turn lies upon layers of collagenous tissue interspersed with mesenchymal cells maintaining the mechanical integrity of the tissue[7]. Interstitial collagens (types I and III) predominate and form parallel bundles of collagen fibrils that produce a scaffold similar in ultrastructual organisation to that seen within the stroma of the cornea[8]. The AM stroma however is considerably thinner than that of the human cornea and, when used therapeutically, the amniotic epithelia are lost and replaced by native corneal epithelia[9]. However, AM stroma can persist in its native form for many months following transplantation under specific conditions[8].

Recently we have shown that there exists a significant variation in structure between different areas of the amniotic sac[10, 11] but despite the increasing use of AM in ophthalmic therapeutic applications there is presently little consideration given to the importance such variation in membrane structure may have on subsequent therapeutic effect, especially clinical transparency. Previously we have investigated the fine structural organisation of collagen fibrils within wounded and normal corneas and successfully related changes in fibril organisation to corneal transparency[12-19]. Thus, considering the previously observed similarities in structure between AM stroma and corneal stroma we have now applied our expertise in understanding corneal transparency to the transparency of clinically relevant AM.

Materials and methods

Collection and storage of human amniotic membrane

Following elective Caesarean section at term, unlinked anonymised samples of amniotic membrane were taken from fetal sac membranes adjoining, but not overlaying the placenta. Fetal membranes overlaying the placenta were not included as they are not commonly used in stem cell transplantation, the technique most strongly associated with the positioning of AM within the visual field for prolonged or indefinite periods. Fetal sac membranes from six patients were collected from the Department of Obstetrics and Gynaecology, Queens Medical Centre, Nottingham, UK, after full local ethics committee approval and in compliance with the Declaration of Helsinki. The fetal membranes were prepared in accordance with a previously published procedure[11]. Firstly, the chorion was separated manually from the amnion and discarded; the remaining AM washed with phosphate-buffered saline (PBS) containing antibiotics (5 ml of 0.5% levofloxacin) to remove blood. Persistent blood

stained AM edges were dissected away and not used. Then under sterile conditions samples (4 cm×4 cm) of AM were taken from areas adjacent to the placental disc (proximal amnion) and approximately 10 cm from the placental disc (distal amnion). These samples were chosen from areas of the AM which were coherent and translucent. The dissected AM samples were stored at −80°C in PBS. These samples were thawed before further examination and subsequently termed freeze-thawed AM. It has previously been confirmed that there is no difference between fresh and frozen AM in terms of clinical efficacy[20].

Four further placentas, providing samples for freeze dried AM, were received either as a gift (Dr T. Nakamura, Kyoto Prefectural University of Medicine, Japan having been prepared according to their published method[21]) or supplied commercially (Acelagraft, Celgene Cellular Therapeutics, NJ).

Transmission measurements.

The freeze-thawed amniotic samples were incubated in Dispase (Gibco) at 37°C for 2 hours and the epithelium removed by scrapping. Both the freeze-thawed and freeze dried samples were incubated in PBS at room temperature for 2 hours before the transmission of light through each sample was measured. Each sample of AM in PBS was flattened and held securely between the two glass plates of a 35mm slide mount. The glass slide mount maintained the AM in a hydrated state with no wrinkles or air bubbles. Each mounted sample was then placed, in turn, within a spectrophotometer (PYE Unicom, SP8-100) and percent transmission was recorded through the visible spectrum (400 – 700 nm). The process was repeated three times for each sample, each time exposing a different area of tissue to the incident light beam. The transmission values were zeroed by subtracting the glass slide mount with PBS alone.

Refractive index measurements.

Following transmission measurements, the refractive index of each AM sample was quantified using a bench-top Abbe 60 Series Refractometer (Bellingham and Stanley Ltd., Tunbridge Wells, England). The refractive index was measured from three different areas of each sample independently by two observers and the average value calculated.

Thickness measurements.

Immediately following transmission measurements a small area (10mm^2) from each sample was embedded in Tissue Tek (Fisher Scientific, UK), snap frozen in liquid nitrogen and stored at -80°C. Cryo-sections (7μm) were then stained with haematoxylin and eosin and thickness measurements across the AM recorded using a calibrated microscope with digital camera (Zeiss, Axioskop 2). To compensate for the natural heterogeneity of AM structure three serial sections were taken from three regions of increasing depth through each embedded sample, ten measurements were taken from each section and the results averaged.

Predicted transparency calculations.

Transparency through corneal stroma can be predicted using an established model, the direct summation of fields for light scattering by fibrils[12, 22, 23]. In this study we applied the same model to predict transparency through corneal stroma with a thickness artificially reduced to that of AM. This facilitated a direct comparison in transmission spectra between the cornea (predicted) and AM (actual) by normalising for tissue thickness. Briefly, assuming there is no absorption, the fraction of light

transmitted undeviated through the cornea is related to the total scattering cross-section per fibril per unit length, σ, by the equation:

$$F(\lambda) = e^{-\rho\sigma t} \quad \text{(Eq 1)}$$

where t is the thickness of the stroma, ρ is the bulk number density of fibrils in the stroma, and σ, the scattering cross-section, is a function of the following, 1) the size of the fibrils 2) the packing of the fibrils, 3) the refractive indices of the hydrated fibrils and hydrated interfibrillar matrix and, 4) wavelength (λ). t was calculated from our light microscopy measurements of AM, the size and packing of corneal collagen fibrils were taken from representative published electron micrographs of human corneal stroma[24] and the refractive index of the fibrils and interfibrillar matrix was taken from previously published data[25].

Results

Light microscopy confirmed that the epithelial cells had been successfully removed from the freeze-thawed AM and that none were present on the surface of freeze-dried AM prior to transmission measurements (Figure 1). The freeze-dried, freeze-thawed distal and freeze-thawed proximal AM had a mean thickness of 21.6μm (sd ± 5.6), 64.3 (sd ± 20.9) and 95.3μm (sd ± 27.9) respectively. The freeze-dried AM was significantly thinner than the freeze-thawed AM ($p < 0.01$, Student's t-Test). Within the freeze-thawed AM samples thickness was significantly greater in areas proximal to the placenta when compared to AM collected from areas distal to the placenta ($p < 0.01$, Student's t-Test) (Figure 2).

Transparency (percent transmission of visible light) differed significantly between the three types of AM investigated (freeze-dried, freeze-thawed proximal and freeze-thawed distal). Transparency increased in line with tissue thickness, the freeze-dried AM (thinnest) having the highest transmission spectra and the freeze-thawed proximal AM (thickest) having the lowest transmission spectra (Figure 3).

The freeze-dried, freeze-thawed distal and freeze-thawed proximal AM had a mean refractive index of 1.335 (sd ± 0.001), 1.334 (sd ± 0.002) and 1.357 (sd ± 0.002) respectively. There was no significant difference between the refractive index of freeze-dried and freeze-thawed distal AM both having a similar refractive index to water (1.333). The refractive index of freeze-thawed proximal AM was significantly higher than the freeze-thawed distal AM ($p < 0.001$, Student's t-Test) and much nearer to the refractive index of the corneal stroma (1.375)[25] (Figure 4).

The direct summation of fields method facilitated a comparison in transparency between corneal tissue of different thicknesses (Figure 5). The values of the thicknesses used were taken from the AM thickness measurements by light microscopy (Figure 2). By comparing the predicted levels of transparency with the actual AM transmission spectra, shown in figure 3, freeze-dried, freeze-thawed distal and freeze-thawed proximal AM were calculated to be 85%, 83% and 68% as transparent as the human cornea respectively once normalised for stromal thickness.

Discussion

The results suggest that significant variations in the optical properties of AM exist. We have shown that preservation and sampling protocol can influence both the transmission of visible light and refractive index of AM used for ocular surface regeneration. The divergence in measured transparency between freeze-dried AM and

freeze-thawed AM, despite having a similar refractive index, is most likely explained by differences in tissue thickness since when normalised for thickness there was very little difference between the subsequent predicted corneal transparencies. However, the relative smoothness of the freeze-dried AM surface and complete absence of epithelial cells would have also reduced the scatter of incident light increasing its transparency.

Interestingly the smallest relative difference in refractive index between human cornea and AM was shown by the freeze-thawed proximal sample. This may have some clinical relevance as the larger the difference in refractive index between cornea and transplanted AM the greater the chance of scatter at the interface between the two tissues would be. If this were the case and despite its lower transparency, freeze-thawed proximal AM may be more suitable for the packing of deep corneal wounds, such as ulcers, especially if we consider that AM can persist unaltered within the corneal stroma for 12 months[8].

Using AM for ocular surface reconstruction within the visual field, tissue taken from an area of the amniotic sac distal to the placenta offers the most transparency. However, freeze dried AM preservation provides an increased level of transparency over a freeze-thaw method of preservation.

Acknowledgements

We would like to acknowledge funding support from the NC3R, Diawa Anglo-Japanese Foundation and JSPS Furusato Award (CJC). KMM is a Royal Society/Wolfson Foundation Merit Award holder.

Competing interest: None declared

Figure legends

Figure 1. Freeze-dried AM lacks the presence of epithelial or stromal cells and is of uniform thickness (A). Freeze-thawed AM is uneven in its thickness, AM collected distal to the placental (B) is thinner than AM collected proximal/adjacent to the placenta (C). Whilst epithelial cells have been successfully removed by enzyme treatment followed by scraping, stromal cells persist (arrows). However these cells are likely to be devitalised following the freeze-thaw process. Scale bars = 20μm.

Figure 2. Thickness measurements of freeze-dried, freeze-thawed distal and freeze-thawed proximal AM were taken from the light micrographs. Proximal AM was significantly found to be the thickest whilst freeze-dried AM was found to be significantly the thinnest. Error bars correspond to standard error.

Figure 3. The percentage transmission of visible light was compared through freeze-dried, freeze-thawed distal and freeze-thawed proximal AM. The freeze-thawed proximal AM has the lowest transmission spectra whereas the freeze-dried had the highest. Error bars correspond to standard error.

Figure 4. Refractive index was compared between freeze-dried, freeze-thawed distal and freeze-thawed proximal AM. No significant difference was observed between freeze-dried and freeze-thawed distal AM, both similar to water. Freeze-thawed proximal AM had a significantly high refractive index than the other types of AM. *The refractive index values of human cornea and water were taken from published data[25]. Error bars correspond to standard error.

Figure 5. Predicted transmission of visible light through cornea at various thicknesses using the direct summation of fields method. The graph clearly shows a decrease in transparency with increasing tissue thickness. Thickness values correspond to the measured thickness of freeze-dried, freeze-thawed distal and freeze-thawed proximal AM. A comparison between these spectra and measured spectra through AM (Figure 3.) facilitates a direct evaluation of transparency between cornea and AM by normalising for tissue thickness.

References

1. Meller D, Pires RT, Tseng SC. Ex vivo preservation and expansion of human limbal epithelial stem cells on amniotic membrane cultures. Br J Ophthalmol 2002;86:463-71.
2. Schwab IR. Cultured corneal epithelia for ocular surface disease. Trans Am Ophthalmol Soc 1999;97:891-986.
3. Koizumi N, Inatomi T, Quantock AJ, Fullwood NJ, Dota A, Kinoshita S. Amniotic membrane as a substrate for cultivating limbal corneal epithelial cells for autologous transplantation in rabbits. Cornea 2000;19:65-71.
4. Gomes JA, Romano A, Santos MS, Dua HS. Amniotic membrane use in ophthalmology. Curr Opin Ophthalmol 2005;16:233-40.
5. Tsai RJ, Li LM, Chen JK. Reconstruction of damaged corneas by transplantation of autologous limbal epithelial cells. N Engl J Med 2000;343:86-93.
6. Moore RM, Mansour JM, Redline RW, Mercer BM, Moore JJ. The Physiology of Fetal Membrane Rupture: Insight Gained from the Determination of Physical Properties. Placenta 2006;In Press, Corrected Proof.
7. Malak TM, Ockleford CD, Bell SC, Dalgleish R, Bright N, Macvicar J. Confocal immunofluorescence localization of collagen types I, III, IV, V and VI and their ultrastructural organization in term human fetal membranes. Placenta 1993;14:385-406.
8. Connon CJ, Nakamura T, Quantock AJ, Kinoshita S. The Persistence of Transplanted Amniotic Membrane in Corneal Stroma. American Journal of Ophthalmology 2006;141:190-192.
9. Nubile M, Dua HS, Lanzini TE-M, et al. Amniotic membrane transplantation for the management of corneal epithelial defects: an in vivo confocal microscopic study. Br J Ophthalmol 2008;92:54-60.
10. Connon CJ, Nakamura T, Hopkinson A, et al. The biomechanics of amnion rupture: an x-ray diffraction study. PLoS ONE 2007;2:e1147.

11. Hopkinson A, McIntosh RS, Tighe PJ, James DK, Dua HS. Amniotic Membrane for Ocular Surface Reconstruction: Donor Variations and the Effect of Handling on TGF-{beta} Content. Invest. Ophthalmol. Vis. Sci. 2006;47:4316-4322.
12. Connon CJ, Marshall J, Patmore AL, Brahma A, Meek KM. Persistent haze and disorganization of anterior stromal collagen appear unrelated following phototherapeutic keratectomy. J Refract Surg 2003;19:323-32.
13. Connon CJ, Meek KM. Organization of corneal collagen fibrils during the healing of trephined wounds in rabbits. Wound Repair Regen 2003;11:71-8.
14. Meek K, Leonard D, Connon C, Dennis S, Khan S. Transparency, swelling and scarring in the corneal stroma. Eye 2003;17:927-36.
15. Connon CJ, Meek KM. The structure and swelling of corneal scar tissue in penetrating full-thickness wounds. Cornea 2004;23:165-71.
16. Connon CJ, Meek KM, Kinoshita S, Quantock AJ. Spatial and temporal alterations in the collagen fibrillar array during the onset of transparency in the avian cornea. Exp Eye Res 2004;78:909-15.
17. Meek KM, Elliott GF, Sayers Z, Whitburn SB, Koch MH. Interpretation of the meridional x-ray diffraction pattern from collagen fibrils in corneal stroma. J Mol Biol 1981;149:477-88.
18. Meek KM, Leonard DW. Ultrastructure of the corneal stroma: a comparative study. Biophys J 1993;64:273-80.
19. Meek KM, Quantock AJ. The use of X-ray scattering techniques to determine corneal ultrastructure. Prog Retin Eye Res 2001;20:95-137.
20. Adds PJ, Hunt CJ, Dart JKG. Amniotic membrane grafts, "fresh" or frozen? A clinical and in vitro comparison. Br J Ophthalmol 2001;85:905-907.
21. Nakamura T, Yoshitani M, Rigby H, et al. Sterilized, freeze-dried amniotic membrane: a useful substrate for ocular surface reconstruction. Invest Ophthalmol Vis Sci 2004;45:93-9.
22. Freund DE, McCally RL, Farrell RA. Direct summation of fields for light scattering by fibrils with applications to normal corneas. Appl Opt 1986;25:2739.
23. McCally RL, Freund DE, Zorn A, et al. Light-scattering and ultrastructure of healed penetrating corneal wounds. Invest Ophthalmol Vis Sci 2007;48:157-65.
24. Komai Y, Ushiki T. The three-dimensional organization of collagen fibrils in the human cornea and sclera. Invest Ophthalmol Vis Sci 1991;32:2244-58.
25. Leonard DW, Meek KM. Refractive indices of the collagen fibrils and extrafibrillar material of the corneal stroma. Biophys J 1997;72:1382-7.

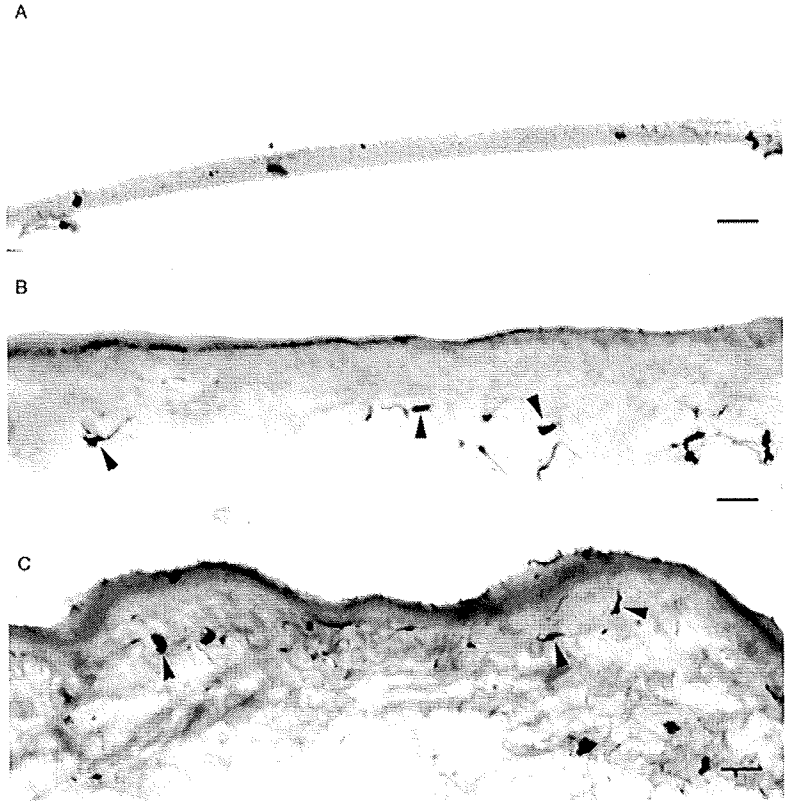

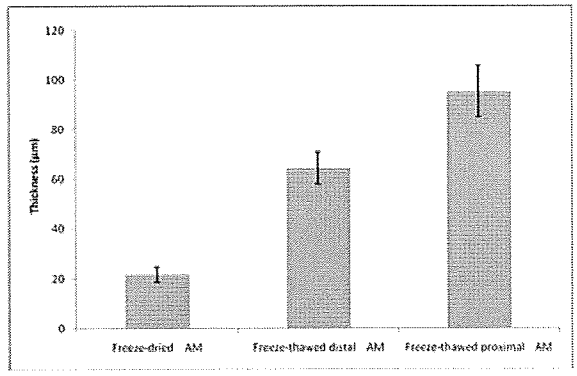

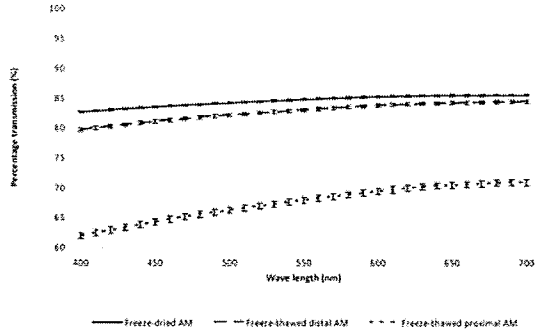

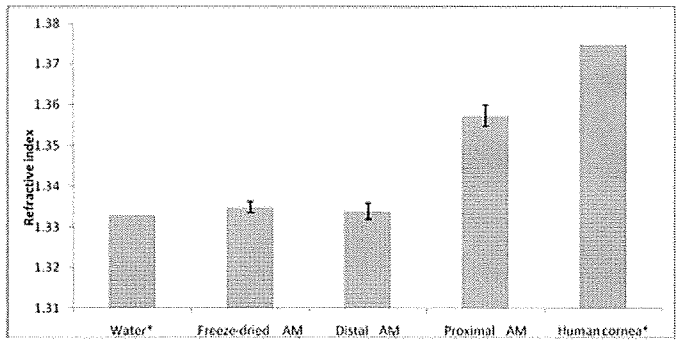

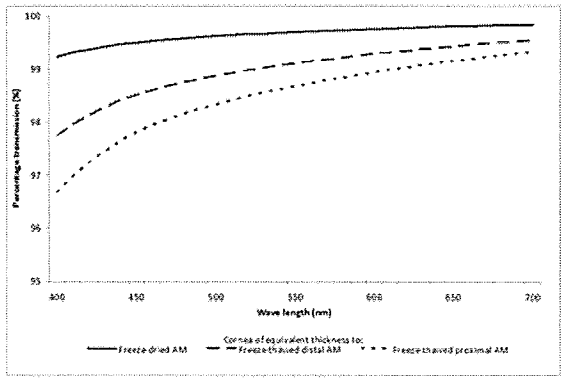

The Role of Interleukin-33 in Chronic Allergic Conjunctivitis

Akira Matsuda,[1,2] *Yoshimichi Okayama,*[3] *Noriko Terai,*[1] *Norihiko Yokoi,*[1] *Nobuyuki Ebihara,*[2] *Hidetoshi Tanioka,*[1] *Satoshi Kawasaki,*[1] *Tsutomu Inatomi,*[1] *Norito Katoh,*[4] *Eiichiro Ueda,*[4] *Junji Hamuro,*[1] *Akira Murakami,*[2] *and Shigeru Kinoshita*[1]

Purpose. The authors discovered a genetic association between the *ST2L* gene and atopy. The *ST2L* gene encodes a membrane-bound functional marker for Th2 cells. Recently, a novel Th2 cytokine, interleukin-33 (IL-33), was discovered to be a specific ligand for *ST2L*. The authors investigated the role of IL-33 in chronic allergic conjunctivitis.

Methods. Immunohistochemical analysis was carried out using giant papillae samples obtained from patients with atopic keratoconjunctivitis. The authors used proinflammatory stimuli to clarify IL-33 mRNA/protein-inducing signals with cultured human conjunctival epithelial cells, fibroblasts, human umbilical vascular endothelial cells, and mast cells. These cells were also used to examine the expression of ST2L (IL-33R). Finally, cultured mast cells were stimulated with recombinant IL-33 (rIL-33) to examine the downstream signals.

Results. The authors found IL-33 protein expression in human vascular endothelial cells in the giant papillae and in the control conjunctivae. IL-33 expression was also observed in conjunctival epithelium of the giant papillae but not in the control conjunctivae. IL-1β stimulation upregulated IL-33 mRNA expression in conjunctival fibroblasts. The authors also confirmed mature IL-33 protein expression in ocular resident cells by Western blot analysis. Preferential ST2L expression was observed in human mast cells, and phosphorylation of p38 MAPK and IL-13 mRNA induction was observed in human cultured mast cells after rIL-33 stimulation. Phosphorylation of p38 MAPK was inhibited by soluble ST2 protein.

Conclusions. The IL-33-ST2 signaling cascade plays some roles in the pathophysiology of chronic allergic conjunctivitis through the activation of mast cells. (*Invest Ophthalmol Vis Sci.* 2009;50:4646-4652) DOI:10.1167/iovs.08-3365

From the Departments of [1]Ophthalmology and [4]Dermatology, Kyoto Prefectural University of Medicine, Kyoto, Japan; [2]Department of Ophthalmology, Juntendo University School of Medicine, Tokyo, Japan; and [3]Division of Molecular Cell Immunology and Allergology, Advanced Medical Research Center, Nihon University Graduate School of Medicine, Tokyo, Japan.

Supported in part by Grants-in-Aid for Scientific Research Programs 19659454 (SKi), 18604009 (AMa), 21592239 (AMa), and 20591195 (YO) from the Japanese Ministry of Education, Culture, Sports, Science and Technology and by the Japanese National Institute of Biomedical Innovation (Project ID05-24) program.

Submitted for publication December 29, 2008; revised April 17, 2009; accepted July 14, 2009.

Disclosure: **A. Matsuda**, None; **Y. Okayama**, None; **N. Terai**, None; **N. Yokoi**, None; **N. Ebihara**, None; **H. Tanioka**, None; **S. Kawasaki**, None; **T. Inatomi**, None; **N. Katoh**, None; **E. Ueda**, None; **J. Hamuro**, None; **A. Murakami**, None; **S. Kinoshita**, None

The publication costs of this article were defrayed in part by page charge payment. This article must therefore be marked "*advertisement*" in accordance with 18 U.S.C. §1734 solely to indicate this fact.

Corresponding author: Akira Matsuda, Department of Ophthalmology, Kyoto Prefectural University of Medicine, 465 Kajii-cho, Hirokoji-agaru, Kawaramachi-dori, Kamigyo-ku, Kyoto 602-0841, Japan; akimatsu@koto.kpu-m.ac.jp.

Our previous study showed a strong genetic association between atopic dermatitis/high serum IgE status and a functional single nucleotide polymorphism (SNP) in the distal promoter region of ST2.[1] The *ST2* gene encodes two molecules by alternative splicing. One molecule is ST2L, which is controlled by the distal promoter and encodes a membrane receptor for a recently discovered Th2 cytokine, interleukin-33 (IL-33).[2] The other molecule is soluble ST2, which works as a decoy receptor for IL-33. The biological activities of IL-33, including IgE induction and eosinophil infiltration to the target tissues, can be explained by the signaling cascade through membrane-bound ST2L (IL-33R/IL-33 receptor), which had been extensively investigated as a marker for Th2 cells.[3,4] Other lines of study showed that the IL-33 precursor is identical to a nuclear factor for high endothelial venule (NF-HEV), which is a gene cloned from high endothelial venule (HEV) tissue,[5] and is identical to *DVS-27*, a gene cloned from rat subarachnoid hemorrhage model.[6]

In this study, we investigated the role of the IL-33/IL-33R signaling cascade in chronic allergic conjunctivitis because IL-33 shares homologous sequences with IL-1, a known proinflammatory cytokine, expressed by ocular surface epithelial cells and plays some roles in allergic conjunctivitis.[7] In addition, IL-33 shares the receptor beta chain (IL-1RAP) with IL-1,[8] indicating that both cytokines may share its downstream signaling cascades.

To elucidate the role of IL-33 in ocular surface inflammation, we examined the in vivo expression of IL-33 protein using biopsy samples obtained from atopic keratoconjunctivitis (AKC),[9] a typical Th2-biased disease; superior limbic keratoconjunctivitis (SLK)[10,11] and Mooren ulcer,[12] models for non-Th2-biased inflammation; and conjunctivochalasis, a noninflammatory control conjunctiva.[13] We found IL-33 protein expression at human vascular endothelial cells and HEV in the conjunctival tissues. In chronic allergic conjunctivitis, IL-33 expression was also observed in the conjunctival epithelium. We also used proinflammatory stimuli to clarify the IL-33-inducing mechanism using cultured cells. IL-1β could upregulate IL-33 mRNA expression in ocular surface epithelial cells and fibroblasts.

Materials and Methods

Reagents, Antibodies, and Plasmids

Rabbit anti-human IL-33 polyclonal antibody was purchased from MBL (Nagoya, Japan), anti-human CD4 and CD31 antibodies were purchased from Dako Japan (Kyoto, Japan), and rat anti-PNAd IgM antibody (clone MECA-79) was purchased from BD Biosciences (Franklin Lakes, NJ). Phospho-p38 MAPK antibody was purchased from Promega (Madison, WI), and total p38 MAPK monoclonal antibody and normal rabbit IgG were purchased from Santa Cruz Biotechnology (Santa Cruz, CA). Recombinant human interferon-gamma (rIFN-γ), recombinant human IL-1β (rIL-1β), and recombinant human IL-33 (rIL-33) were purchased from PeproTech (London, UK).

Investigative Ophthalmology & Visual Science, October 2009, Vol. 50, No. 10

Immunohistochemistry

Immunofluorescence staining was performed to examine the expression of IL-33, CD4, CD31 (endothelial cell marker), and PNAd (HEV marker) in the giant papillae obtained from six patients with AKC and the control conjunctival tissues (obtained from five patients with conjunctivochalasis, four with SLK, and two with Mooren ulcer). Detailed information for the patients (with AKC, SLK, and conjunctivochalasis) has been described elsewhere.[14] Cryosections (7 μm) were fixed in 4% paraformaldehyde in phosphate-buffered saline (PBS) and then stained with rabbit anti-IL-33, mouse anti-CD31, and rat anti-PNAd antibodies (BD Bioscience). We also immunostained sections from four skin biopsy samples obtained from patients with atopic eczema. The sections were then scanned with a confocal microscope (FV-1000; Olympus Corporation, Tokyo, Japan). Negative control specimens were immunostained with normal rabbit IgG antibody instead of rabbit anti-IL-33 antibody. Double immunostaining was carried out on pairs of the anti-IL-33 antibody with the mouse anti-CD31 antibody or with the rat anti-PNAd antibody. Donkey Alexa 488-conjugated anti-rabbit IgG antibody, donkey Alexa 594-conjugated anti-mouse IgG antibody, and donkey Alexa 594-conjugated anti-rat IgG antibody (all from Invitrogen Japan, Tokyo, Japan) were used as secondary antibodies. All procedures were approved by the ethics committee of Kyoto Prefectural University of Medicine, and the study was conducted in accordance with the tenets of the Declaration of Helsinki.

Cell Culture and Stimulation with rIL-1β

The immortalized human conjunctival epithelial (HCJE) cell line was kindly provided by Ilene K. Gipson.[15] Cultured human primary conjunctival fibroblasts were prepared and maintained as previously described.[16] Conjunctival epithelial cells/fibroblasts were stimulated with rIL-1β (10 ng/mL) and rIL-1β + rIFN (10 ng/mL) for 24 hours. The HCJE cell line was cultured with defined keratinocyte serum-free growth medium (Invitrogen Japan). Conjunctival fibroblasts were cultured with 10% fetal calf serum in Dulbecco's minimum essential medium (Invitrogen Japan). Human umbilical vascular endothelial cells (HUVECs) were obtained from DS Pharma Biomedical (Osaka, Japan) and were cultured with human vascular endothelial culture medium according to the manufacturer's protocol. The human mast-cell line LAD2 was kindly provided by Arnold Kirshenbaum (National Institute of Allergy and Infectious Diseases, National Institutes of Health) and was maintained as previously described.[17] HUVECs and LAD2 were also stimulated with rIL-1β (10 ng/mL) for 24 hours.

Reverse Transcription and Real-Time PCR Analysis

With the use of an RNA purification kit (RNeasy; Qiagen Japan, Tokyo, Japan), total RNA was isolated from cultured cells (conjunctival epithelial cells and fibroblasts). cDNA was made with a reverse transcriptase (ReverTra-Ace; Toyobo, Osaka, Japan) using random hexamers according to manufacturer's protocol. Real-time PCR probes and primers specific for human IL-1β (Hs00174097_m1), human IL-33 (Hs00369211_m1), human IL-13 (Hs00174379_m1), human IL-1 receptor alpha (IL-1R1;Hs00991010_m1), human ST2L (Hs00249389_m1), and human 18S-rRNA were purchased from Applied Biosystems (Assay on Demand Products; Applied Biosystems Inc., Foster City, CA). Real-time PCR analysis was performed with a detection system (ABI PRISM 7300 HT Sequence; Applied Biosystems). Relative expression of IL-33 in the cultured cells was quantified by the standard curve method, and relative expression of IL-1β, IL-1R, IL-13, and ST2L was quantified by comparative Ct methods using 18S-rRNA expression in the same cDNA as the controls. The standard curve was made with pCRII-IL-33 plasmid prepared by PCR-based subcloning.

SDS-Polyacrylamide Gel Electrophoresis and Western Blot Analysis

HCJE cells and fibroblasts were collected and washed twice with phosphate-buffered saline (PBS), and the number of cells was counted. Cells (2×10^4) were then solubilized in SDS-sample buffer (62.5 mM Tris-HCl, pH 6.8, 2% SDS, 20% glycerol, and 0.04% bromophenol blue). Next, 50 mM dithiothreitol was added to the samples and incubated for 15 minutes at 65°C. Of each sample, 15 μL was loaded onto 12% Tris-glycine gel with prestained protein standards (Precision Blue; Bio-Rad Japan, Tokyo, Japan). The electrophoresed protein was transferred to polyvinylidene fluoride (PVDF) membrane (Pall Japan, Tokyo, Japan). The membrane was then incubated with rabbit anti-human IL-33 polyclonal antibody (a 1:500 dilution in 1% nonfat skim milk) overnight at 4°C. After washing with Tris-buffered saline (10 mM Tris-HCl, pH 7.6, 150 mM NaCl) containing 0.05% Tween 20 (TBS-T), the membrane was incubated with a 1:10,000 dilution of horseradish peroxidase-conjugated anti-rabbit IgG (GE Healthcare, Uppsala, Sweden) for 1 hour and was visualized with Western blotting reagents (ECL Plus; GE Healthcare).

Reporter Gene Assay

ST2L (the membrane-bound form of ST2) or soluble ST2 (sST2) were overexpressed in HCJE cells with the pBOS-human ST2L expression vector or the pEF6-human sST2 vector, respectively, as previously described.[18] Mock transfection was carried out with empty pBOS vectors. Forty-eight hours after transfection, pNFκB promoter plasmids (Stratagene Japan, Tokyo, Japan) and the pRL-TK vector (Promega) were cotransfected into the HCJE cells. The pRL-TK vectors served as an internal control for transfection efficiency into the epithelial cells. All transfections were carried out with reagent (Lipofectamine LTX; Invitrogen Japan). Twenty-four hours after reporter gene transfection, each sample was stimulated with rIL-33 (50 ng/mL), rIL-1 (10 ng/mL), or PBS only. Twenty-four hours after cytokine stimulation, luciferase activity was measured (Dual Luciferase Reporter Assay Kit, Promega)

Quantification of Relative IL-1R and ST2L (IL-33R) Expression

Real-time PCR analysis was carried out using cDNA obtained from unstimulated HCJE cells, conjunctival fibroblasts, HUVECs, and mast cells.

Mast Cell Stimulation with rIL-33 and Downstream Signal Analysis

To analyze the rIL-33-induced phosphorylation of p38 MAPK, LAD2 cells (2×10^4 cells/well in a 24-well dish) were stimulated with rIL-33 (50 ng/mL) for 15 minutes. As control experiments, neutralization of rIL-33 was carried out by the addition of anti-ST2 antibody (clone 2A5; MBL) or recombinant soluble ST2 (R&D Systems, Minneapolis, MN). Western blot analysis was carried out using phosphospecific p38 mitogen-activated protein kinase (MAPK) and total p38 MAPK antibodies. IL-13 mRNA expression in LAD2 cells, with rIL-33 (50 ng/mL) or rIL-1β (10 ng/mL) stimulation for 6 hours and 24 hours, was also quantified by real-time PCR, as described.

Results

Immunohistochemistry of Giant Papillae

IL-33 immunohistochemical staining with rabbit anti-human IL-33 polyclonal antibody was carried out on giant papillae samples obtained from patients with AKC (Figs. 1, 2A–D). IL-33 immunostaining was observed in $PNAd^+$ HEV cells (Fig. 1C, arrowheads), though not all the $IL\text{-}33^+$ cells were $PNAd^+$ (Fig. 1C, arrows). Negative control staining using control rabbit IgG showed no definite staining (Fig. 1D). $IL\text{-}33^+$ immunostaining could be observed in vascular endothelial cells (Fig. 2) and in some part of the epithelial cells (Figs. 2A, 2C) and fibroblasts (Fig. 2D, asterisks) of giant papillae. Double immunostaining with anti-CD4 antibody showed that the $IL\text{-}33^+$ vascular endothelial cells were surrounded by $CD4^+$ T cells (Fig. 2B, arrow). Double immunostaining with anti-CD31 antibody con-

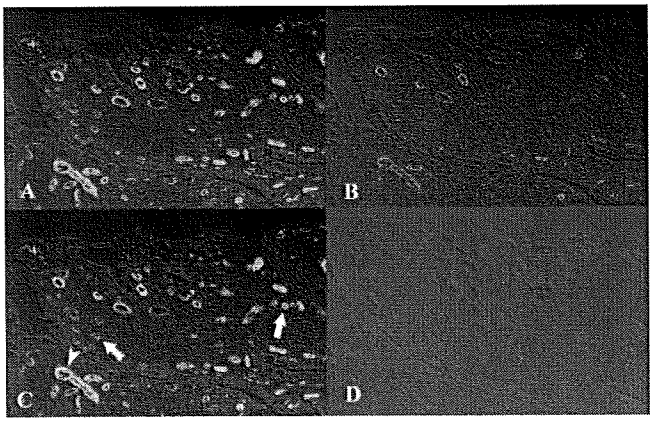

FIGURE 1. Immunohistochemical analysis of giant papillae using rabbit anti-human IL-33 antibody. Giant papillae obtained from a patient with AKC were immunostained with the anti-IL-33 antibody (**A**). The same slides were also immunostained with anti-PNAd (HEV) monoclonal antibody (**B**). The merged image is shown (**C**). *Arrows*: PNAd$^-$ IL-33 staining. *Arrowhead*: IL-33$^+$ HEV. Negative control staining of the adjacent section with normal rabbit IgG is shown (**D**). Original magnification, 200×.

firmed positive IL-33 staining in vascular endothelium (Fig. 2C). Nuclear IL-33$^+$ staining was observed in some vascular endothelial cells (Fig. 2C, arrowhead). On the other specimens, cytoplasmic IL-33 staining was observed in vascular endothelial cells (Fig. 2D, arrows), and fibroblasts were also positive for IL-33 staining (Fig. 2D, asterisks). A skin biopsy section obtained from a patient with atopic dermatitis showed positive IL-33 immunostaining in epithelium and vascular endothelium (Fig. 2F).

IL-33 immunostaining was also observed in vascular endothelium of conjunctivae obtained from a patient with conjunctivochalasis (Fig. 2E), a patient with SLK (Fig. 3A), and the nuclei of HEV in conjunctival tissue obtained from a patient with Mooren ulcer (Figs. 3B, 3C). However, no definitive IL-33$^+$ staining was observed in the epithelial cells or in the fibroblasts of the conjunctivae obtained from those patients.

IL-1β Stimulation Induced IL-33 mRNA Expression in HCJE/Conjunctival Fibroblasts

IL-33 mRNA expression in HCJE cells and fibroblasts was quantified with real-time PCR. In human HCJE cells, the induction of IL-33 mRNA expression was 1.2-fold by IL-1β stimulation and 1.4-fold by IL-1β + IFN-γ stimulation. The overall magnitude of IL-33 mRNA expression was greater in conjunctival fibroblasts than in conjunctival epithelial cells, and 16-fold IL-33 mRNA induction was observed by IL-1β stimulation. No IL-33 mRNA expression was observed in cultured human mast cells. On the other hand, IL-1β treatment reduced constitutive IL-33 mRNA expression in HUVECs (Fig. 4A). For the purpose of comparison, relative IL-1β mRNA expression was also quantified by real-time PCR. HCJE cells showed the most abundant IL-1β mRNA expression. IL-1β mRNA induction was observed in conjunctival fibroblasts and HUVECs. Only a negligible amount of IL-1β mRNA expression was detected in mast cells (Fig. 4B).

IL-33 Western Blot Analysis

Western blot analysis was carried out with rabbit anti-human IL-33 polyclonal antibody using HCJE lysate and conjunctival fibroblast lysate, both stimulated with rIL-1β or rIL-1β + IFN-γ for 24 hours. In the case of fibroblasts, a marked increase of pro-IL-33 was observed after stimulation (Fig. 5, arrow). No definitive bands corresponding to pro-IL-33 molecular weight (30 kDa, arrow) were observed in HCJE cells. A modest amount of mature IL-33 protein was observed in HCJE cells and conjunctival fibroblasts, but no increase of mature IL-33 protein was observed with rIL-1β treatment (Fig. 5, asterisk). No additive effect for rIL-1β + IFN-γ stimulation was observed for IL-33 expression.

ST2L (IL-33R)–Dependent NF-κB Activation in HCJE

HCJE cells were transfected with the ST2L (IL-33R) expression vector or the sST2 (a decoy receptor for IL-33) expression vector. NF-κB activation by IL-1β stimulation was observed in all samples examined (Fig. 6A). ST2L-transfected HCJE cells showed a higher NF-κB activation signal than did those of mock-transfected HCJE or sST2-transfected cells (Fig. 6A).

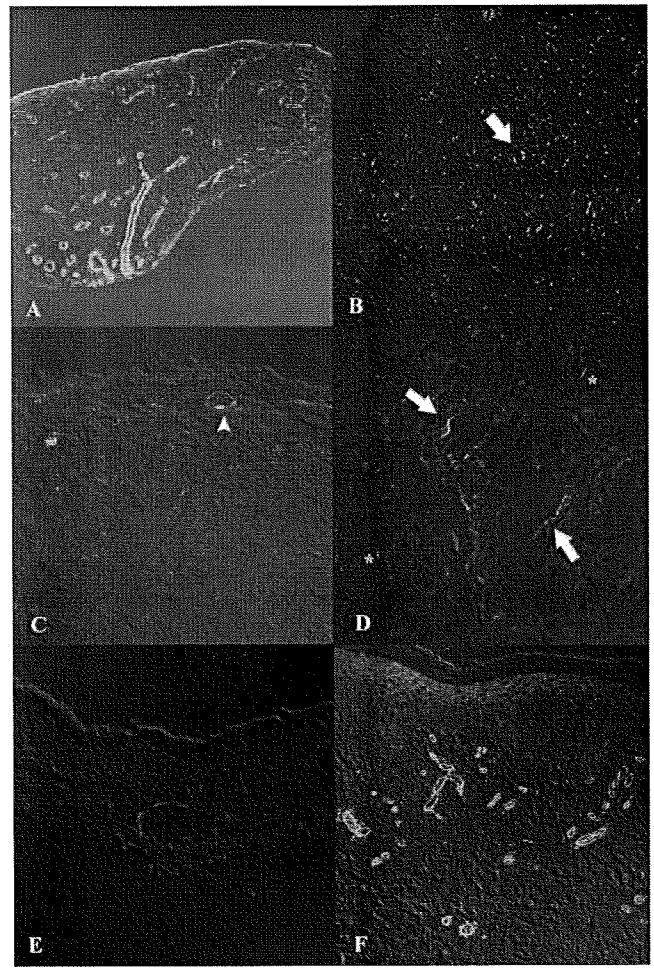

FIGURE 2. Immunohistochemical analysis of giant papillae using anti-human IL-33 antibody. Giant papillae obtained from patients with AKC were immunostained with anti-IL-33 polyclonal antibody (**A**) and double immunostained with anti-IL-33 and anti-CD4 monoclonal antibody (**B**). *Arrow*: IL-33$^+$ vascular endothelium surrounded by CD4$^+$ T cells. (**C**) Double-immunostained with anti-IL-33 and anti-CD31 monoclonal antibody. *Arrowhead*: nuclear IL-33 staining in the vascular endothelium. (**D**) Cytoplasmic IL-33 staining in the vascular endothelium (*arrows*); IL-33$^+$ fibroblastic staining (*asterisks*). (**E**) Control conjunctiva obtained from a patient with conjunctivochalasis. Positive IL-33 immunostaining was observed in the vascular endothelium. (**F**) IL-33 immunostaining of a skin biopsy specimen of a patient with atopic eczema. Positive staining was observed in the epithelium and vascular endothelium. Original magnifications, 200× (**A**, **B**, **F**); 400× (**C**–**E**).

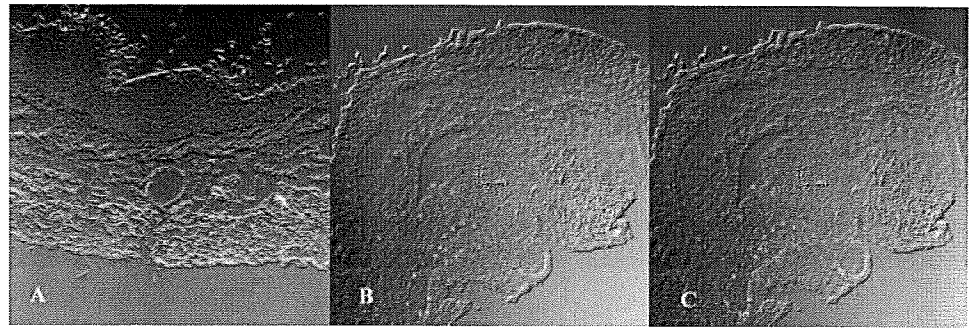

FIGURE 3. Immunohistochemical staining of conjunctival specimens obtained from patients with SLK or Mooren ulcer using anti-IL-33 antibody. Frozen sections made from conjunctival specimens obtained from a patient with SLK (**A**) and a patient with Mooren ulcer (**B**, **C**) were stained by polyclonal anti-IL-33 antibody. Nuclear IL-33 staining was observed in the vascular endothelium. Double immunostaining was carried out with anti-PNAd (HEV) antibody (**C**). Original magnification, 200×.

IL-1R and ST2L (IL-33R) Receptor Expression Levels Are Distinct among the Cell Types

The relative mRNA expression of IL-1R and ST2L was quantified by real-time PCR. Abundant IL-1R mRNA expression was observed in HCJE cells and conjunctival fibroblasts, whereas a negligible amount of IL-1R expression was observed in mast cells. On the other hand, abundant ST2L mRNA expression was observed in mast cells but not in HCJE cells or conjunctival fibroblasts. HUVECs showed modest IL-1R and ST2L mRNA expression (Fig. 6B).

Mast Cell Stimulation with rIL-33–Induced p38 MAPK Activation and IL-13 Upregulation

Human mast cell line LAD2 was stimulated with rIL-33 for 5, 15, and 30 minutes, and phosphospecific p38 MAPK immunoblotting was then carried out. Prominent p38 phosphorylation was observed 15 minutes after rIL-33 stimulation (Fig. 7A). IL-13 mRNA expression in rIL-33–stimulated LAD2 cells was quantified with real-time PCR analysis. Relative magnitude of IL-13 mRNA expression was shown. Marked IL-13 induction was observed in rIL-33–stimulated LAD2 cells but not in rIL-1β–stimulated mast cells (Fig. 7B).

DISCUSSION

Immunohistologic analysis of ocular tissue showed constitutive IL-33 expression in vascular endothelial cells (Figs. 1–3). These results are consistent with previous reports that showed IL-33 expression at vascular endothelial cells in human colon, lung, liver, and skin tissue.[19] We found IL-33$^+$ HEV at the stromal region of the giant papillae (Fig. 1C, arrowhead). Given that the IL-33 molecule was originally cloned from HEV by differential display,[5] it is reasonable that we found IL-33$^+$ HEV cells in our samples. It is reported that HEV cells are abundant in the T-cell zone of lymphatic tissue, and they play a major role in lymphocyte homing to lymphatic tissue.[20] Our results also showed that IL-33$^+$ vascular cells were surrounded by CD4$^+$ T cells (Fig. 2B, arrow). Because of the preferential ST2L (IL-33R) expression in Th2 cells compared with Th1 cells,[3,4] IL-33$^+$ HEV cells may play a role in the activation and infiltration of Th2 lymphocytes, as suggested by previous reports.[21,22]

IL-33 protein expression is observed not only in the nucleus of endothelial cells (Fig. 2C, arrowhead), as reported in previous reports,[19,23] but also in the cytoplasm in some vascular endothelial cells (Fig. 2D, arrows). Given that the IL-33 nuclear localization signal is located at the N-terminal of the pro-IL-33 protein,[24] it is reasonable that it is expressed in cytoplasm, at least in mature IL-33 protein, in which N-terminal amino acid sequences were cleaved by caspase-1.[2] Based on these results, we theorize that nuclear and cytoplasmic IL-33 expression is possible in conjunctival tissue, and nuclear IL-33 localization suggests the existence of the pro-IL-33 protein.

In the giant papillae of patients with AKC and in skin biopsy specimens obtained from patients with atopic eczema, positive IL-33 staining was observed not only in the vascular endothelium but also in epithelial cells (Figs. 2A, 2C, 2F). On the other hand, IL-33 expression is restricted to the vascular endothelium of conjunctivae of patients with conjunctivochalasis (Fig. 2E), SLK (Fig. 3A), and Mooren ulcer (Figs. 3B, 3C). We used conjunctivae samples obtained from patients with conjunctivochalasis as noninflammatory control conjunctivae, as shown previously.[13] Although we analyzed only a limited number of samples, extravascular IL-33 protein expression might be one

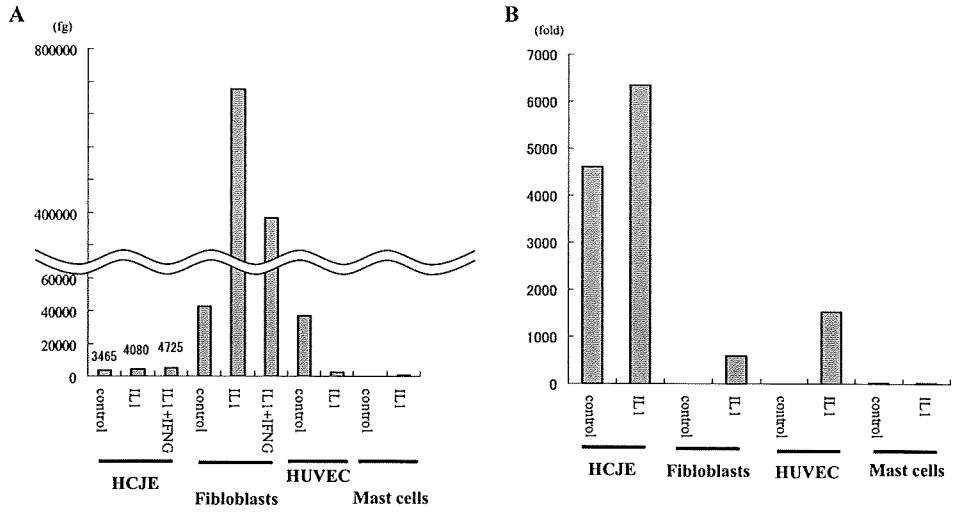

FIGURE 4. Real-time PCR analysis of IL-33 mRNA expression using cultured cells with IL-1β stimulation. HCJE cells, conjunctival fibroblasts, HUVECs, and mast cells were stimulated with rIL-1β (10 ng/mL) for 24 hours (**A**). HCJE cells and fibroblasts were also stimulated with rIL-1β + rIFN-γ (10 ng/mL). After total RNA extraction and reverse transcription, real-time PCR analysis was carried out. The standard curve was made with the IL-33-pCRII dual promoter plasmid (1000 = 1 pg plasmid). Relative IL-1β mRNA expression was quantified using the same cDNA samples (**B**). The relative amount of IL-1β mRNA was shown by fold changes using the IL-1β expression in unstimulated HUVECs as standard. These results are representative of three independent experiments.

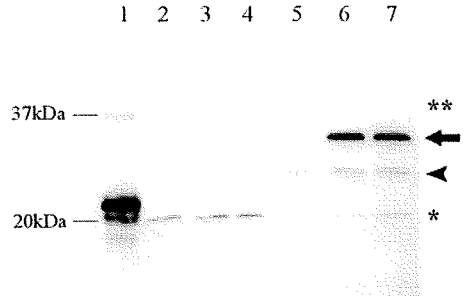

FIGURE 5. Immunoblotting analysis of IL-33 protein using HCJE cells and fibroblasts. Cultured conjunctival epithelial cells and fibroblasts were stimulated with rIL-1β (10 ng/mL) and rIL-1β + rIFN-γ (10 ng/mL) for 24 hours. Western blot analysis was carried out using rabbit anti-human IL-33 polyclonal antibody. The molecular weight of mature IL-33 protein was approximately 20 kDa (*asterisk*), whereas for the proform of IL-33 protein it was approximately 30 kDa (*arrow*). An additional band of unknown origin was observed around 27 kDa (*arrowhead*). A proposed dimeric form of IL-33 protein was observed around 40 kDa (*double asterisks*). *Lane 1*, rIL-33 (100 ng); *lanes 2–4*, conjunctival epithelial cells; *lanes 5–7*, conjunctival fibroblasts; *lanes 2* and *5*, no stimulation; *lanes 3* and *6*, rIL-1β stimulation; *lanes 4* and *7*, rIL-1β + rIFN-γ stimulation.

of the pathologic elements of chronic allergic disease. Because Leonardi et al.[25] reported that IL-1β protein was expressed in 4 of 6 tear samples obtained from patients with vernal keratoconjunctivitis (VKC; average, 21.7 pg/mL) but not in any of the tear samples obtained from controls, it is possible that the tears of AKC and VKC patients induce extravascular IL-33 expression at the ocular surface.

We next tried to detect proinflammatory stimuli to induce IL-33 expression. A previous report showed that the IL-33 (DVS-27) gene is induced prominently by IL-1β and moderately by IFN-γ in human artery smooth muscle cells.[6] We then stimulated HCJE cells, corneal fibroblasts, HUVECs, and mast cells with IL-1β for 24 hours and found that IL-33 mRNA was induced by rIL-1β stimulation in HCJE cells and conjunctival fibroblasts. Our result was consistent with previous results for IL-33 induction in dermal fibroblasts by a combination of IL-1β/TNF-α.[2] A weak additive effect for rIL-1β + IFN-γ costimulation was observed in the mRNA level. On the other hand, IL-33 mRNA expression was suppressed in HUVECs by the same IL-1β. This result is consistent with the previous results by Kuchler et al.[23] that showed IL-33 downregulation by IL-1 stimulation. We also examined IL-1β mRNA expression using the same cDNA samples (Fig. 4B) and found that constitutive IL-1β mRNA expression was observed in HCJE cells and that IL-1β mRNA expression was induced in conjunctival fibroblasts and in HUVECs with the stimulation of IL-1β itself. Interestingly, the reverse kinetics of IL-33 mRNA and IL-1β mRNA expression was observed in IL-1β–stimulated HUVECs (Fig. 4A vs. 4B). We considered that the reverse kinetics was not contradictory because the loss of constitutive IL-33 expression in the nucleus may activate transcriptional machinery in HUVECs, as has been shown in other reports.[23] As a result of our in vivo and in vitro experiments, we agree with the theory proposed by Carriere et al.[24] that IL-33 may work as a dual-function protein (a nuclear protein with repressive properties and as a proinflammatory cytokine) and other types of dual-function proteins such as IL-1α[26] and HMGB1.[27]

As a next step, we tried to detect IL-33 protein because it was reported that caspase-1–dependent cleavage is required for mature IL-33.[2] Immunoblotting experiments showed clear induction of the pro-IL-33 molecule in response to rIL-1β stimulation for 24 hours in conjunctival fibroblasts (Fig. 5, lanes 5 and 6, arrow); however, no definitive increase in mature IL-33 was observed (Fig. 5, lanes 5 and 6, asterisk). No additive effect for IL-33 protein induction was observed with IL-1β + IFN-γ simulation compared with the effect of IL-β stimulation (Fig. 5, lanes 4 and 7).

In the case of HCJE cells, the induction of pro-IL-33 protein was not observed in contrast to that of conjunctival fibroblasts (Fig. 5, lanes 2 and 3, arrow); however, a comparable amount of mature IL-33 expression was observed (Fig. 5, lanes 2 and 3 vs. lanes 5 and 6, asterisk). A previous report showed caspase-1 protein expression in ocular surface epithelial cells.[28] These results might be attributed to the more efficient IL-33 maturation process by caspase-1 in conjunctival epithelial cells compared with fibroblasts. The origin of higher molecular weight bands around 40 kDa (Fig. 5, double asterisks) observed in HCJE cells and in rIL-33 is unknown, but they might be a dimeric form of IL-33. Our immunohistologic results showed that some of the epithelial cells (Figs. 2A, 2C) and some of the fibroblastic cells (Fig. 2D) in the giant papillae were IL-33$^+$. Further studies are essential to elucidate IL-33 protein maturation and subcellular localization.

We then attempted to find the effector cells for IL-33 among ocular surface resident cells. At first we examined HCJE cells because it is known that IL-1 stimulation may activate these cells through the IL-1R signaling cascade.[29,30] Our result showed that ST2L transfection is required for NF-κB activation in response to IL-33 in HCJE cells (Fig. 6A), which means that the amount of ST2L expression is a determinant factor for the responsiveness against IL-33. Therefore, we examined ST2L

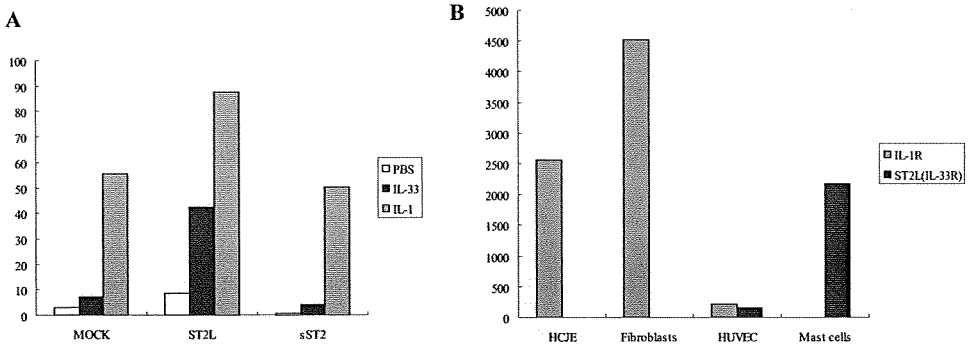

FIGURE 6. Receptor amount-dependent responses against rIL-1β or rIL-33. The reporter gene assay ST2L (IL-33R) or soluble ST2 (sST2; a decoy receptor for IL-33) were overexpressed in conjunctival epithelial cells using the pBOS-ST2L expression vector or the pEF6-sST2 vector, respectively (A). Forty-eight hours after transfection, pNFκB and pRL-TK (internal control) reporter plasmids were cotransfected into the HCJE cells. Twenty-four hours after reporter gene transfection, each sample was stimulated with rIL-33 (50 ng/mL), rIL-1 (10 ng/mL), or PBS only. Twenty-four hours after stimulation, luciferase activity was measured. Results show the representative data of five independent experiments. (B) IL-1R and IL-33R expression. IL-1R and ST2L (IL-33R) mRNA was quantified by real-time PCR analysis using cDNA made from HCJE cells, conjunctival fibroblasts, HUVECs, and human mast cells. Relative mRNA expression was shown by fold changes using mast cells (for IL-1R) and HCJE (for ST2L) as standards. Results show the representative data of three independent experiments.

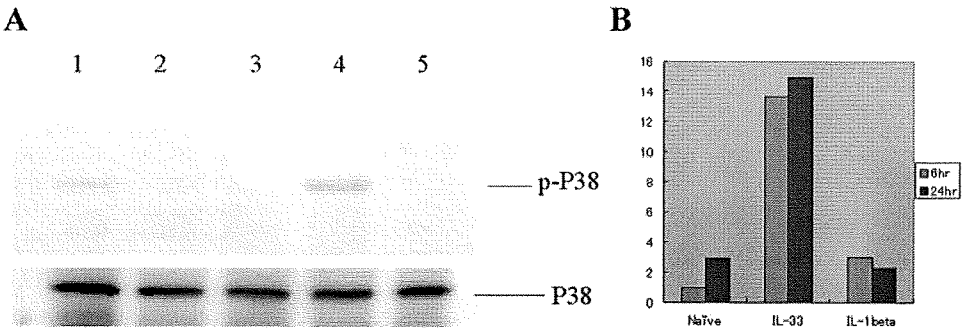

FIGURE 7. Mast cell stimulation with rIL-33-induced phosphorylation of p38 MAPK and IL-13 mRNA expression. (**A**) Human mast cell line LAD2 (2×10^4 cells/well in a 24-well dish) was stimulated with rIL-33 (50 ng/mL) for 15 minutes. Control experiments include anti-ST2 antibody + rIL-33 (*lane 1*), recombinant soluble ST2 + rIL-33 (*lane 2*), recombinant soluble ST2 + rIL-33 (preincubated in tube; *lane 3*), rIL-33 only (*lane 4*), and PBS (*lane 5*). Western blot analysis was carried out using phosphospecific p38 MAPK and total p38 MAPK antibodies. (**B**) IL-13 mRNA expression in LAD2 cells after rIL-33 (50 ng/mL) or rIL-1β (10 ng/mL) stimulation for 16 hours. After total RNA extraction, real-time PCR analysis was carried out. This result is representative of three independent experiments.

mRNA expression level by real-time PCR and found that ST2L (IL-33R) mRNA is abundantly expressed in human mast cells but not in HCJE or fibroblasts (Fig. 6B). Based on these results, we considered that the human mast cell is a good candidate to be an effector cell of IL-33.

Consistent with the results of previous studies,[31-33] we found that rIL-33 could activate the p38 MAPK signaling cascade (Fig. 7A) and could induce IL-13 mRNA expression in human mast cells (Fig. 7B). Neutralizing experiments showed that the sST2 molecule could completely inhibit rIL-33–mediated p38 MAPK activation and that anti-ST2 antibody could partially inhibit p38 MAPK activation (Fig. 7A). This result suggests that the sST2 molecule may have a therapeutic value for allergic diseases, as suggested by the mouse asthma model.[18] It should also be noted that the ability of rIL-33 to induce IL-13 mRNA expression in mast cells was far stronger than that of rIL-1β (Fig. 7B). Based on these results we considered that the ratio of IL-1R1/IL-33R expression depends on the cell types (Fig. 6B) and that it may have some functional significance.

In summary, we found in vivo IL-33 protein expression in epithelium and vascular endothelium of the giant papillae in patients with severe chronic allergic conjunctivitis. We also found IL-1β–induced IL-33 mRNA expression and pro-IL-33 protein expression, particularly in the cultured conjunctival fibroblasts. The IL-33-ST2L (IL-33R) signaling cascade may play some role in the pathophysiology of chronic allergic conjunctivitis through the activation of mast cells. Further investigations are essential to elucidate the molecular mechanism of IL-33 expression control and its role in atopic disease.

Acknowledgments

The authors thank Ilene K. Gipson for providing the HCJE cell line, Arnold Kirshenbaum for providing the LAD2 cell line, Morisada Hayakawa and Shinichi Tominaga for providing expression vectors, Hisako Takeshita for excellent technical assistance, and John Bush for English language editing.

References

1. Shimizu M, Matsuda A, Yanagisawa K, et al. Functional SNPs in the distal promoter of the ST2 gene are associated with atopic dermatitis. *Hum Mol Genet.* 2005;14:2919-2927.
2. Schmitz J, Owyang A, Oldham E, et al. IL-33, an interleukin-1-like cytokine that signals via the IL-1 receptor-related protein ST2 and induces T helper type 2-associated cytokines. *Immunity.* 2005;23:479-490.
3. Yanagisawa K, Naito Y, Kuroiwa K, et al. The expression of ST2 gene in helper T cells and the binding of ST2 protein to myeloma-derived RPMI8226 cells. *J Biochem.* 1997;121:95-103.
4. Xu D, Chan WL, Leung BP, et al. Selective expression of a stable cell surface molecule on type 2 but not type 1 helper T cells. *J Exp Med.* 1998;187:787-794.
5. Baekkevold ES, Roussigne M, Yamanaka T, et al. Molecular characterization of NF-HEV, a nuclear factor preferentially expressed in human high endothelial venules. *Am J Pathol.* 2003;163:69-79.
6. Onda H, Kasuya H, Takakura K, et al. Identification of genes differentially expressed in canine vasospastic cerebral arteries after subarachnoid hemorrhage. *J Cereb Blood Flow Metab.* 1999;19:1279-1288.
7. Keane-Myers AM, Miyazaki D, Liu G, Dekaris I, Ono S, Dana MR. Prevention of allergic eye disease by treatment with IL-1 receptor antagonist. *Invest Ophthalmol Vis Sci.* 1999;40:3041-3046.
8. Chackerian AA, Oldham ER, Murphy EE, Schmitz J, Pflanz S, Kastelein RA. IL-1 receptor accessory protein and ST2 comprise the IL-33 receptor complex. *J Immunol.* 2007;179:2551-2555.
9. Foster CS, Rice BA, Dutt JE. Immunopathology of atopic keratoconjunctivitis. *Ophthalmology.* 1991;98:1190-1196.
10. Corwin ME. Superior limbic keratoconjunctivitis. *Am J Ophthalmol.* 1968;66:338-340.
11. Matsuda A, Tagawa Y, Matsuda H. Cytokeratin and proliferative cell nuclear antigen expression in superior limbic keratoconjunctivitis. *Curr Eye Res.* 1996;15:1033-1038.
12. Brown SI. What is Mooren's ulcer? *Trans Ophthalmol Soc U K.* 1978;98:390-392.
13. Yokoi N, Komuro A, Nishii M, et al. Clinical impact of conjunctivochalasis on the ocular surface. *Cornea.* 2005;24:S24-S31.
14. Matsuda A, Okayama Y, Ebihara N, et al. Hyperexpression of the high-affinity IgE receptor-β chain in chronic allergic keratoconjunctivitis. *Invest Ophthalmol Vis Sci.* 2009;50:2871-2877.
15. Gipson IK, Spurr-Michaud S, Argueso P, Tisdale A, Ng TF, Russo CL. Mucin gene expression in immortalized human corneal-limbal and conjunctival epithelial cell lines. *Invest Ophthalmol Vis Sci.* 2003;44:2496-2506.
16. Kawasaki S, Nishida K, Sotozono C, Quantock AJ, Kinoshita S. Conjunctival inflammation in the chronic phase of Stevens-Johnson syndrome. *Br J Ophthalmol.* 2000;84:1191-1193.
17. Kirshenbaum AS, Akin C, Wu Y, et al. Characterization of novel stem cell factor responsive human mast cell lines LAD 1 and 2 established from a patient with mast cell sarcoma/leukemia; activation following aggregation of FcåRI or FcγRI. *Leuk Res.* 2003;27:677-682.
18. Hayakawa H, Hayakawa M, Kume A, Tominaga S. Soluble ST2 blocks interleukin-33 signaling in allergic airway inflammation. *J Biol Chem.* 2007;282:26369-26380.
19. Moussion C, Ortega N, Girard JP. The IL-1-like cytokine IL-33 is constitutively expressed in the nucleus of endothelial cells and epithelial cells in vivo: a novel 'alarmin'? *PLoS ONE.* 2008;3:e3331.
20. Kraal G, Mebius RE. High endothelial venules: lymphocyte traffic control and controlled traffic. *Adv Immunol.* 1997;65:347-395.
21. Smithgall MD, Comeau MR, Yoon BR, Kaufman D, Armitage R, Smith DE. IL-33 amplifies both Th1- and Th2-type responses through its activity on human basophils, allergen-reactive Th2 cells, iNKT and NK cells. *Int Immunol.* 2008;20:1019-1030.
22. Komai-Koma M, Xu D, Li Y, McKenzie AN, McInnes IB, Liew FY. IL-33 is a chemoattractant for human Th2 cells. *Eur J Immunol.* 2007;37:2779-2786.
23. Kuchler AM, Pollheimer J, Balogh J, et al. Nuclear interleukin-33 is generally expressed in resting endothelium but rapidly lost upon

angiogenic or proinflammatory activation. *Am J Pathol.* 2008;173:1229–1242.

24. Carriere V, Roussel L, Ortega N, et al. IL-33, the IL-1-like cytokine ligand for ST2 receptor, is a chromatin-associated nuclear factor in vivo. *Proc Natl Acad Sci U S A.* 2007;104:282–287.
25. Leonardi A, Borghesan F, DePaoli M, Plebani M, Secchi AG. Procollagens and inflammatory cytokine concentrations in tarsal and limbal vernal keratoconjunctivitis. *Exp Eye Res.* 1998;67:105–112.
26. Werman A, Werman-Venkert R, White R, et al. The precursor form of IL-1α is an intracrine proinflammatory activator of transcription. *Proc Natl Acad Sci U S A.* 2004;101:2434–2439.
27. Lotze MT, Tracey KJ. High-mobility group box 1 protein (HMGB1): nuclear weapon in the immune arsenal. *Nat Rev Immunol.* 2005;5:331–342.
28. Solomon A, Rosenblatt M, Li DQ, et al. Doxycycline inhibition of interleukin-1 in the corneal epithelium. *Invest Ophthalmol Vis Sci.* 2000;41:2544–2557.
29. Moore JE, McMullen TC, Campbell IL, et al. The inflammatory milieu associated with conjunctivalized cornea and its alteration with IL-1 RA gene therapy. *Invest Ophthalmol Vis Sci.* 2002;43:2905–2915.
30. Narayanan S, Corrales RM, Farley W, McDermott AM, Pflugfelder SC. Interleukin-1 receptor-1-deficient mice show attenuated production of ocular surface inflammatory cytokines in experimental dry eye. *Cornea.* 2008;27:811–817.
31. Iikura M, Suto H, Kajiwara N, et al. IL-33 can promote survival, adhesion and cytokine production in human mast cells. *Lab Invest.* 2007;87:971–978.
32. Allakhverdi Z, Smith DE, Comeau MR, Delespesse G. Cutting edge: the ST2 ligand IL-33 potently activates and drives maturation of human mast cells. *J Immunol.* 2007;179:2051–2054.
33. Ho LH, Ohno T, Oboki K, et al. IL-33 induces IL-13 production by mouse mast cells independently of IgE-FcåRI signals. *J Leukoc Biol.* 2007;82:1481–1490.

Blue light and near-infrared fundus autofluorescence in acute Vogt-Koyanagi-Harada disease

Hideki Koizumi, Kazuichi Maruyama and Shigeru Kinoshita

Br J Ophthalmol published online December 3, 2009
doi: 10.1136/bjo.2009.164665

BJO Online First, published on December 3, 2009 as 10.1136/bjo.2009.164665

Blue light and near-infrared fundus autofluorescence in acute Vogt-Koyanagi-Harada disease

Hideki Koizumi, MD, PhD, Kazuichi Maruyama, MD, PhD, and Shigeru Kinoshita, MD, PhD

From the Department of Ophthalmology, Kyoto Prefectural University of Medicine, Kyoto, Japan

Correspondence to: Hideki Koizumi, MD, PhD, 465 Kajii-cho, Kamigyo-ku, Kyoto 602–0841, Japan; Tel: (81) 75-251-5578; Fax: (81) 75-251-5663;
E-mail: hidekoiz@koto.kpu-m.ac.jp

Running Title: Autofluorescence in acute VKH disease

Key Words: Vogt-Koyanagi-Harada disease, Blue light fundus autofluorescence, Near-infrared fundus autofluorescence, Choroid, Retinal pigment epithelium

Word Count: 1926 words

Presented in part at the Association for Research in Vision and Ophthalmology (ARVO) Annual Meeting, Ft. Lauderdale, Florida, May 7, 2009.

The authors have no commercial or proprietary interest in products mentioned in the article.